Soft Matter

Cite this: *Soft Matter*, 2012, **8**, 6471

www.rsc.org/softmatter

PAPER

Phase behavior of gradient copolymer solutions: a Monte Carlo simulation study

Gunja Pandav,[a] Victor Pryamitsyn,[a] Keith C. Gallow,[b] Yueh-Lin Loo,[b] Jan Genzer[c] and Venkat Ganesan*[a]

Received 13th March 2012, Accepted 16th April 2012
DOI: 10.1039/c2sm25577d

We use computer simulations to study the phase separation behavior of amphiphilic linear gradient copolymer solution under poor solvent conditions. Using the bond fluctuation model and parallel tempering algorithm, we explore the influence of the gradient strength (the largest difference in the instantaneous composition along the copolymer) upon the phase separation characteristics. Under poor solvent conditions, the chains collapse to form micelle-like aggregates. We find that the critical temperature for this transition exhibits a linear dependence on the gradient strength of the copolymers. A systematic quantification of the cluster characteristics formed during the phase separation also reveals a strong dependence of aggregation numbers and the bridging statistics upon the gradient strength of the copolymers. Analysis of our results reveals that the critical parameter determining the thermodynamic behavior of gradient copolymers is in fact the average length of the hydrophobic sequences in the gradient copolymers. We demonstrate that the latter provides a useful measure to quantitatively predict the critical transition temperature of the gradient copolymer solution. We also present a few results from the framework of an annealed representation of the sequences of the gradient copolymer to demonstrate the limitations arising from such a model representation.

1 Introduction

With the development of advanced polymerization techniques, it is now becoming possible to exercise significant control over polymer properties by controlling their physicochemical characteristics such as molecular weight, chain architecture, sequence chemistry *etc.*[1–4] As a consequence, synthesis of new classes of copolymers, such as gradient copolymers, comb copolymers, star copolymers *etc.*, is now becoming common.[5–8] In this study we focus on a class of such polymers, which has recently attracted significant attention in the context of interfacial modifiers, termed *gradient copolymers*.[9–14] Gradient copolymers are random copolymers which exhibit a gradual change in monomer composition along the length of the polymer.[15,16] A number of other uses have also been proposed for such a class of polymers, which include applications as reinforcement agents,[17] damping materials[18] and thermoplastic elastomers.[19 20]

The equilibrium properties of gradient copolymers are expected to be intermediate between the behavior of diblock copolymers, which exhibit a step change in composition, and that of random copolymers, which possess a uniform composition profile.[21–24] For instance, Okabe *et al.*[21,22] observed micelle formation and microphase segregation in a semi-dilute aqueous solution of gradient copolymers and block copolymers using small-angle neutron scattering and dynamic light scattering (DLS). The micelle size for gradient copolymers was found to decrease gradually with temperature and less ordered micelle structures were observed as compared to block copolymer solutions. The work reported in the present article is motivated by recent experimental results of Gallow *et al.*[25,26] which examined the effect of monomer sequence distribution on the cloud point of dilute solutions of gradient copolymers. They synthesized a series of 2-hydroxyethyl methacrylate and 2-(dimethylamino)ethyl methacrylate gradient copolymers having pre-specified composition profiles. In dilute aqueous-buffered solutions, these copolymers exhibited aggregation and phase separation phenomena whose onset was sensitively dependent on the details of monomer sequence distribution. Moreover, based on the combined results of DLS and cloud point observations, a two-step aggregation mechanism for solutions was proposed, in which the initial stages of phase separation involves the local collapse of the chains (intramolecular aggregation) followed by strong inter-chain aggregation which manifests as macroscopic clouding.

A number of prior theoretical studies have considered the phase behavior of gradient copolymer systems, but mostly in the regime of melt-like conditions.[27–32] Such studies have examined the interfacial properties,[33] the self-assembly morphologies[27–32] and the conformations of polymer brushes[34] using polymer self consistent field theory. Despite this significant body of literature,

[a]*Department of Chemical Engineering, University of Texas at Austin, Austin, TX 78712, USA. E-mail: venkat@che.utexas.edu*
[b]*Department of Chemical and Biological Engineering, Princeton University, Princeton, NJ 085441, USA*
[c]*Department of Chemical and Biomolecular Engineering, North Carolina State University, Raleigh, NC 27695, USA*

the phase behavior of gradient copolymers in solution conditions remains unexplored. In the present work, we report results of Monte Carlo (MC) simulation studies exploring the phase behavior of gradient copolymer solutions. Our work seeks to address the influence of the sequence distribution of the gradient copolymers upon their phase separation characteristics in poor solvent conditions. To quantify the phase separation characteristics, we examine the size and organization of the clusters formed during phase separation and quantify the relative roles of inter and intramolecular aggregation. Specifically, we would like to address: (i) the origin of the gradient strength dependence of the critical temperature; and (ii) whether the sequence of aggregation events indeed correspond to that hypothesized in experiments.

A second, related issue we probe in this study is the influence of the "randomness" of the gradient copolymer sequences. Specifically, many of the prior theoretical studies[27–31,34] have used an "annealed" representation of the gradient copolymer (albeit, exceptions do exist[32]). In such a model, all the copolymers are assumed to possess the same sequence with, however, the identity and the interactions of each monomer chosen to be representative of the "averaged" identity of the monomer. While this is a reasonable first step, a more realistic model for such systems, and one that we primarily focus on in this work, is to use an ensemble of "quenched" sequences, whose compositions on an average mimic the experimentally synthesized conditions of the gradient copolymers. For instance, recent work has demonstrated that the chemical sequence of copolymer compatibilizers can significantly influence the dynamics of phase separation of immiscible binary homopolymer blends.[14] Other studies[35–38] have demonstrated that the use of the more realistic quenched sequences for grafted copolymers can lead to novel phenomena and effects which cannot in general be captured by the annealed sequences. Motivated by such considerations, we compare the phase separation characteristics of annealed sequences with the behavior of the more realistic, quenched sequence model of gradient copolymer systems.

The rest of this article is arranged as follows. In Section 2, we outline details of our simulation methodology, the quenched and annealed models of the linear gradient copolymer systems and the framework used for cluster analysis. In Section 3, we present our results in both the annealed and quenched systems for the phase transition temperature and the characteristics of the micelle-like structures formed below the phase separation temperature. We discuss our results in connection with the above-cited experimental observations.

2 Simulation details

2.1 Bond fluctuation model

MC lattice models have been used extensively to study the equilibrium properties for a variety of copolymeric systems.[14,32,39–50] In this specific work, we use the bond fluctuation method (BFM) of Carmesin and Kremer[51] to study the phase separation process in gradient copolymer solutions.[52] Many prior studies have demonstrated BFM simulation approach as a convenient method to study both the equilibrium and dynamical properties of polymer melts and solutions. For instance, earlier studies have applied the BFM approach for the study of issues such as phase separation of polymer blends,[53] interdiffusion of polymers,[51] the static and dynamical properties of block copolymers[54] and the transport properties of penetrants in polymer matrices.[55,56]

In BFM, a polymer chain is represented by cubes (each monomer occupying 8 lattice sites) on a lattice, with a maximum occupancy for each lattice position restricted to a single monomer in order to model excluded volume interactions. The monomers are connected by bond vectors whose magnitudes l lie in the range $2 \leq l \leq 10$. The latter constrains the bond vectors to the set [200][210][211][221][300][310] and their permutations and sign inversions. An elementary move in BFM consists of choosing a monomer at random and displacing it by one lattice unit. If the move leads to a bond vector contained in the admissible bond vector set and if excluded volume conditions are satisfied, the move is accepted according to the Metropolis criterion based on the energetic differences.[57] The original BFM simulation limits the MC moves only among the 6 directions around the monomer to ensure bond non-crossability. However, we use a modified version of the BFM algorithm proposed by Wittmer *et al.*[58] where attempts to displace the monomer are effected in the 26 available directions. Such a modification helps in reducing the relaxation time for the system, and is especially convenient for probing equilibrium properties.

2.2 Modeling linear gradient copolymer solutions

We consider linear gradient copolymers comprising A (hydrophilic) and B (hydrophobic) monomers. The average compositions of such linear gradient copolymers are modeled through a continuous composition function $c(t)\mathrm{d}t$, where t (index along polymer backbone) varies from 0 to 1. Explicitly,

$$c(t) = 2(f_{\mathrm{A}} - \mathrm{d}x)t + \mathrm{d}x, \quad (1)$$

where f_{A} is the average of composition over the chain, $\mathrm{d}x = f - \Delta g/2$ represents the lowest composition of A monomer and Δg is the gradient strength of the copolymer and is defined as the largest difference in the instantaneous composition along the backbone of copolymer.[25] The composition profile of such linear gradient copolymer is pictorially depicted in Fig. 1(a).

In the experiments discussed in the introduction,[25,26] gradient copolymers were synthesized by a semi batch polymerization process wherein one monomer is loaded and the comonomer flow rate is continuously monitored. While the monomeric sequences generated by the experiments are expected to possess complex correlations along the chain, in an effort to account for the chain-to-chain variability in the sequences, we adopt a stochastic approach relying on an ensemble of many chains to mimic the compositional profiles depicted in Fig. 1(b). Explicitly, for each chain, a specified monomer t is probabilistically chosen to be as either an A or a B monomer based on the average composition at that location. Since the average composition changes along the backbone, the chemical identity of the specified monomers also varies gradually along the backbone (albeit, in a probabilistic manner). To contrast with the phase behavior of random copolymer solutions, we also consider the behavior of a pure random copolymer solution (denoted as R in our results).

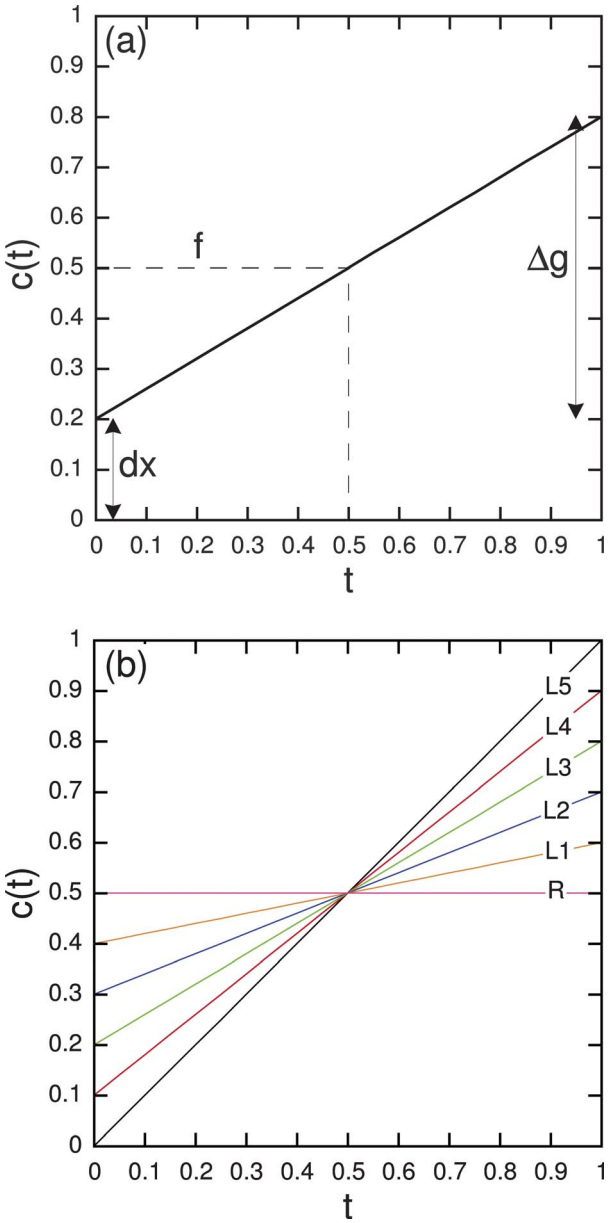

Fig. 1 (a) A depiction of the linear composition profiles adopted for the polymer chains in our simulation. The figure also defines the gradient strength, Δg, a quantity which constitutes the focus of our study. (b) Composition Profiles: R ($\Delta g = 0$), L1 ($\Delta g = 0.2$), L2 ($\Delta g = 0.4$), L3 ($\Delta g = 0.6$), L4 ($\Delta g = 0.8$), L5 ($\Delta g = 1.0$).

In the latter, the polymer chains are populated by a random, uncorrelated sequence of A and B monomers.

To study the phase behavior of a system of above copolymers in solution conditions, we treat the solvent molecules (S) in an implicit manner as the "vacancies" or holes in our system. Following the parametrization of Khokhlov *et al.*,[41] we set both ε_{AB} and ε_{AA} identically to zero, where ε_{ij} refers to the interaction energy parameter between i and j species. In other words, we limit A–A and A–B interactions to just the excluded volume steric interactions. To mimic the hydrophilic and hydrophobic behaviors of the A and B monomers, we impose $\varepsilon_{AS} < 0$, $\varepsilon_{BS} > 0$ and $\varepsilon_{BB} < 0$. Two non-bonded monomers are considered to be interacting if their distance vectors belongs to the set (2,0,0) ∪ (2,1,0) ∪ (2,1,1) (and their permutations and sign inversions) which covers 54 lattice sites around the randomly selected monomer. The maximum number of monomer–monomer contacts for this interaction range is 26, whereas the number of corresponding monomer–solvent contacts is 98. Consequently, we use the following simple parametrization and assume that $-98/26\varepsilon_{AS} = 98/26\varepsilon_{BS} = -\varepsilon_{BB} = \varepsilon$, where ε represents a measure of temperature in the system and constitutes the parameter that is varied in our study. The interaction parameter, ε is proportional to inverse temperature in the case of systems exhibiting upper critical solution temperature (UCST) behavior. However, the experimental results of Gallow *et al.*[25,26] correspond to a lower critical solution temperature (LCST) system. To avoid confusion while comparing the simulation results with experiments, we identify ε to be proportional to temperature, although the same analysis can be easily extended to UCST systems.

All our simulations were carried out for a chain length corresponding to the number of monomers N set to $N = 128$, and for the case where the volume fraction of the polymer chains corresponded $\phi = N \times m \times 8/L^3 \approx 0.03$, where m is the number of copolymer chains of length N. Moreover, we fixed the average composition of the A and B monomers as $f_A = f_B = 0.5$. Our study is primarily concerned with the influence of the "gradient strength" upon the phase separation behavior of copolymer solutions. For this purpose, we study the phase separation behavior of five linear gradient copolymers which are depicted in Fig. 1(b) and are labeled in the increasing order of gradient strengths. Henceforth in this article, we will use the terminology L1–L5 (Fig. 1(b)) to identify the system to which the results correspond.

As mentioned in the introduction, a second objective of this work is to examine the impact of using an annealed model representation of the gradient copolymer solutions. In pursuit of this, we consider the two extreme compositional profiles, L1 and L5 in Fig. 1(b), and consider an annealed representation of the sequences. In this framework, the monomers are not identified as either an A or a B monomer. Instead, each monomer is assumed to be partially A and B with a fraction specified by the composition profile. The interaction energies experienced by a monomer t is then calculated as:

$$E_t = c(t)\left(-\frac{98}{26}\varepsilon_{AS}n_s\right) + (1-c(t))\left(\frac{98}{26}\varepsilon_{BS}n_s - \varepsilon_{BB}\sum_{i=1}^{M}(1-c_i(t))\right), \quad (2)$$

where n_s denotes the number of solvent molecules and M labels the polymeric monomers present in the interaction range of the monomer t. In the above, $c(t)$ denotes the probability of the monomer t being A (*cf.* Fig. 1(a)).

2.3 Parallel tempering algorithm

To study the phase separation behavior of the gradient copolymer solutions in computer simulations, we employed a parallel tempering (PT) algorithm (replica exchange).[59] Many earlier studies[43–45] have demonstrated that PT provides an efficient approach to sample the phase space and acquire better statistics

during polymer collapse and phase separation processes. In this methodology, M non-interacting replicas of the system are simulated in parallel at different temperatures. After a pre-specified number of MC steps within the given temperature, (in this work, PT moves were performed at a frequency of one PT move per one hundred MC sweeps of the system), a swap move is attempted between the configurations of neighboring replicas. Such swap moves are accepted based on the Metropolis criterion:[60]

$$p(t_i \leftrightarrow t_{i+1}) = min\{1, \exp[-(\beta_i - \beta_{i+1})(U_i - U_{i+1})]\} \quad (3)$$

where

$$\beta_i = 1/k_B T_i \quad (4)$$

where U_i is the total energy of the replica system at the temperature T_i. Exchange of configurations between replicas offers an efficient way to overcome the energy barriers encountered at low temperatures and thereby facilitates the system to reach equilibrium.

In our work, we used a modified PT algorithm to make the algorithm efficient for parallel computing. Explicitly, in PT, the only inter-processor communication occurs while attempting a swap. In Message Passing Interface (MPI) implementation, a master thread randomly chooses the replicas which will participate in exchange and broadcasts the information to all threads. This involves global synchronization, a procedure which is computationally expensive. Instead, we implement a decentralized parallel tempering algorithm[61] using SPRNG 4.0 (Scalable Parallel Random Number Generator) library.[62] The SPRNG library provides independent random number streams for parallel processes which are deterministic and reproducible. Thus identical random number streams (starting with same seed) can be spawned on each processor to decide which replicas are participating in the swap. The latter eliminates global synchronization and thus speeds up computation. In addition to these global random number streams (restricted to replica exchange moves), we need to maintain independent random number streams local to the processor to determine Metropolis acceptance for MC moves. The pertinent details of the algorithm have been provided elsewhere.[61]

We use $M = 36$ replicas for our simulations. As we are interested in the collapse and phase separation transition, we mainly focus on the temperature regime around the phase separation temperature of the system. The M replicas are first equilibrated for 1×10^6 MC cycles to get the initial configurations, and then subsequently, parallel tempering is carried out for 5×10^6 MC cycles. The system is further equilibrated for 2×10^6 MC cycles and various thermodynamic quantities are averaged each 100 MC cycles for 3×10^6 MC cycles.

2.4 Cluster analysis algorithm

At low temperatures, amphiphilic gradient copolymers are expected to exist in a homogeneous disordered state in solution. However, upon increasing the temperature, there is expected to be an enhancement in the B–S repulsion and the A–S and B–B attractions. These features are expected to lead to a high temperature state wherein the B monomers of the different chains aggregate to form micelle-like structures. In the snapshots displayed in Fig. 2, such considerations are indeed seen to be borne out in our simulations. Interestingly, bigger clusters are seen to be formed in the case of L5 (highest gradient strength) (Fig. 2 (a)), compared to the L1 (Fig. 2(c)) sequences. These microsegregated structures are not strictly micelles as they lack the typical core-shell structure due to the linear composition profile, but for brevity of notation henceforth we address these structures as micelles.

To compare and contrast (pictorially) the behavior of the quenched sequence model with that of the annealed sequences, we also display the snapshots for the high temperature structures in annealed sequences in Fig. 2(b) and Fig. 2(d). For clarity, annealed sequences are colored in a manner such that the monomers when $c(t) > 0.5$ are identified as B whereas when $c(t) > 0.5$ the monomers are identified as A. In comparing the results in Fig. 2(b) and Fig. 2(d) with Fig. 2(a) and Fig. 2(c), we observe that the annealed model displays structures that are substantially different from the quenched model. Specifically, for the annealed case, the sizes of clusters are seen to increase with decreasing gradient strength, which is opposite to the behavior noted for the quenched model. These results can be understood by noting that for the symmetric case ($f_A = f_B = 0.5$) considered in this study, lowering the gradient strength would render the annealed copolymer system similar to a homopolymer system retaining only the attractions between the hydrophobic monomers (*cf.* Section 2.1). Such interactions would lead to the formation of macroscopic aggregates instead of micelles in the case of annealed L1 polymers, which is consistent with the observed trends in the sizes of the clusters.

A specific objective of this work is to quantify the characteristics of the aggregates (micelles) formed during the phase separation processes in gradient copolymer solutions. In situations involving regular multiblock copolymer solutions, identification of "micelles" proves straightforward since all the hydrophobic monomers are expected to be confined to the core. In such cases, labeling the B monomers and identifying their connectivities would serve to quantify the micellar size and numbers. In contrast, in quenched gradient copolymers, due to the linear composition profiles along the backbone (and the stochastic nature of sequences), there is expected to be a non-zero fraction of hydrophobic monomers which exist outside the "core" of the micelle. To illustrate this feature, in Fig. 3(a), we display a snapshot of the collapsed structures formed during the phase separation of quenched gradient copolymers L5 ($\Delta g = 1$). It is clearly evident that there are B monomers present outside the cores of the micelles in the case of gradient copolymers.

To overcome the above issue and identify the micelles formed during the phase separation of gradient copolymers, we employ a two step procedure by adapting connectivity and cluster identification algorithms used in our prior studies.[63–66] Explicitly, we identify the connectedness between monomers based on whether the monomers are nearest neighbors of each other. To discard the non-core B monomers, we first identify the *biggest cluster in each chain* and identify the monomers in this cluster temporarily as the core of a micelle. As the second step, we color all the other B monomers connected to these micelle cores. To accomplish the latter step, we identify all B monomers which

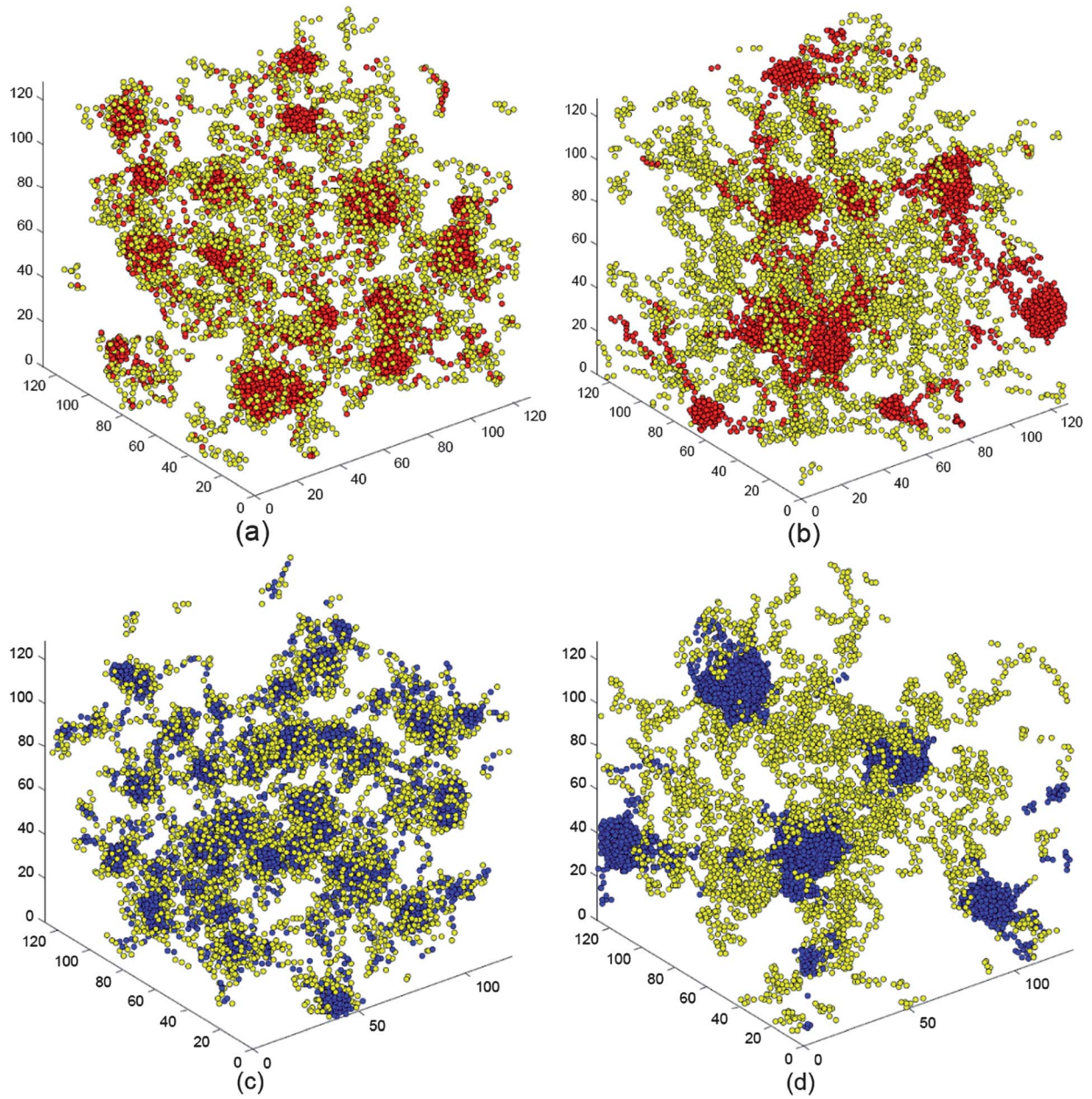

Fig. 2 (a) L5 at $\varepsilon = 0.7$ ($\Delta g = 1.0$) quenched model (b) L5 at $\varepsilon = 0.7$ ($\Delta g = 1.0$) annealed model; Snapshots at (c) L1 at $\varepsilon = 1.0$ ($\Delta g = 0.2$) quenched model (d) L1 at $\varepsilon = 1.7$ ($\Delta g = 0.2$) annealed model.

fall in the interaction range of already colored monomers. The latter is achieved by an iterative process to ensure that every monomer belonging to the interaction range of colored monomers is included. In Fig. 3(b) we depict the cores of micelles identified by this procedure. Our approach correctly identifies the micellar structures while eliminating the non core B monomers. Subsequently, we quantify the statistics of the identified clusters and study their dependencies upon the gradient strengths.

For structures employing annealed sequences, the B monomers cannot be recognized explicitly, since each monomer is partially A and partially B. Thus, we identify the *biggest cluster in each chain* irrespective of whether the monomers are A or B. Then we color all the monomers (A and B) connected to these clusters. This approach correctly captures the onset of interchain aggregation which is one of the main objectives of this study. However, as a consequence of this coloring process, much higher aggregation numbers are expected for the annealed sequences as compared to that of the quenched sequences.

3 Results and discussion

In this section, we present a quantitative discussion of the results of our computer simulation studies. Our specific parametric studies were motivated by recent experiments which examined the phase separation characteristics of gradient copolymers as a function of the gradient strength.[25,26] Inspired by the results of the experimental study we address the following issues:

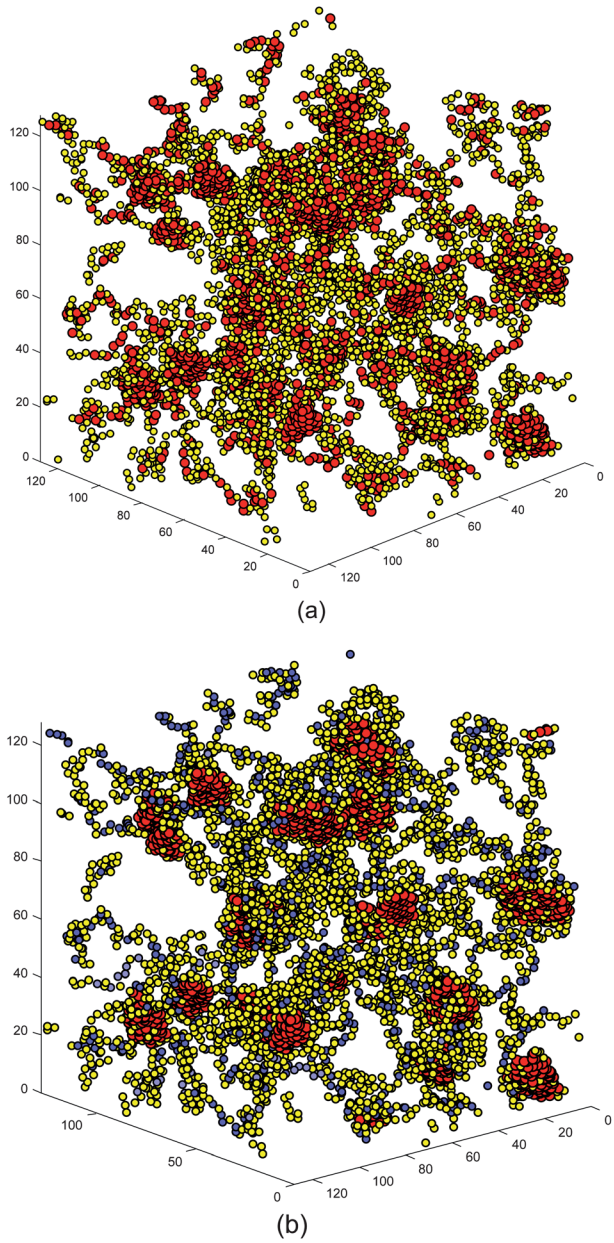

Fig. 3 (a) Snapshots of collapsed micellar structure for L5 ($\Delta g = 1$). The hydrophilic monomers (in yellow color) are intentionally pictured smaller than hydrophobic monomers so as to make it easier to identify micelle cores. (b) Same system with the core of the micelles identified using proposed algorithm. The monomers discarded as a consequence of not belonging to the clusters are indicated by blue color.

(i) Is it possible to define a specific temperature for the transition from the low temperature disordered phase to the high temperature micellar phase? If so, how does the transition temperature depend upon the gradient strength? This issue has arisen from the experimental results which found that the cloud point discerned in the experiments exhibited a linear dependence on the gradient strength of the copolymers.

(ii) What is the sequence of aggregation events accompanying the transition between the low and high temperature phases? Specifically, we are interested in probing the onset of intra- and intermolecular aggregation and their dependence on gradient strength.

(iii) How do the size, number and other characteristics of the micellar structures formed during the phase separation of the system depend on the gradient strength?

(iv) To what extent can the annealed model of sequences capture the behavior predicted by the more realistic, quenched model?

3.1 Phase transition temperature

To quantify the transition from the low temperature to the high temperature phase, we probed the temperature dependence of both the average internal energy and the average fluctuations in the internal energy of the system in our simulations (Fig. 4 and Fig. 5). From Fig. 4(a), we observe that upon increasing the

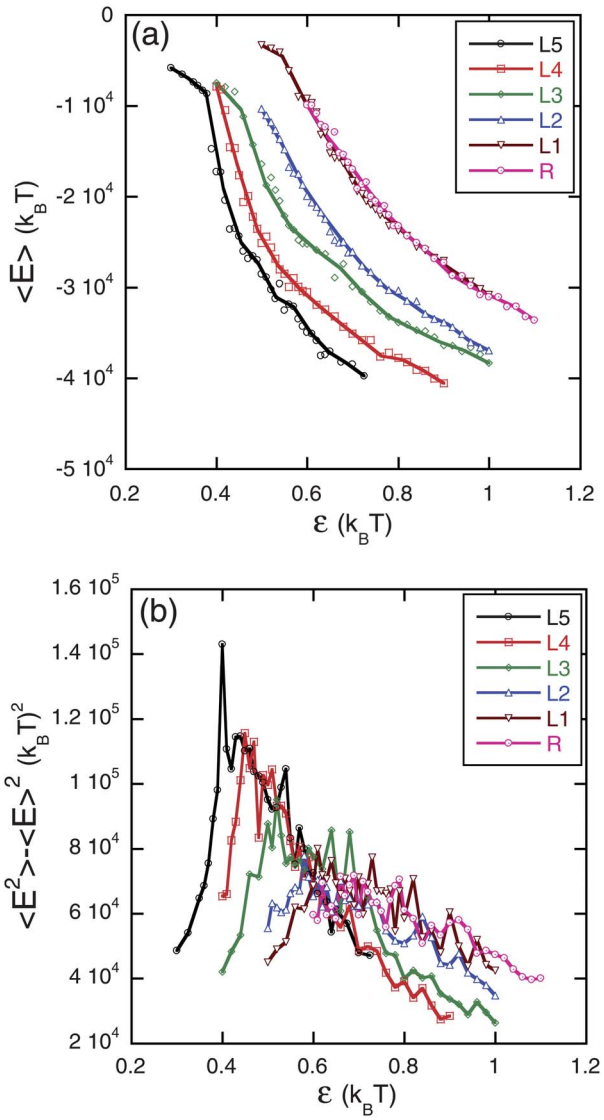

Fig. 4 Quenched model: (a) average energy and (b) average fluctuations in energy as a function of interaction parameter ε: R ($\Delta g = 0$), L1 ($\Delta g = 0.2$), L2 ($\Delta g = 0.4$), L3 ($\Delta g = 0.6$), L4 ($\Delta g = 0.8$), L5 ($\Delta g = 1.0$). Lines are just a guide to the eye.

temperature the system undergoes a steep, albeit continuous, decrease in energy signifying the formation of collapsed micellar phases at high temperatures. More pertinently, we observe that the energy fluctuations in the system (Fig. 4(b)) display a peak at a specific interaction strength, which indicates a transition to an aggregated phase at a critical interaction strength.[39,43,44] A similar trend in energy and energy fluctuations are also observed for simulations employing annealed sequences (Fig. 5(a) and Fig. 5(b)). We note that due to the finite size of the chains used in our simulations, our results for the critical interaction strength are expected to depend on the chain length N of the copolymers. Moreover, for the same reason our results are not sufficient to draw conclusions regarding the order of the phase transition occurring in these systems. Despite these limitations, the peaks in the energy fluctuations are discernible for almost all cases; hence, we use the corresponding temperature (ε_c) as a measure of the phase transition temperature in the system. Furthermore, in the following section, we present results for the temperature dependence of the intermolecular aggregation and micelle sizes, wherein it will be demonstrated that such quantities also undergo a sharp transition at ε_c, thereby confirming that ε_c, as deduced through the energy fluctuations, can be identified as the phase transition temperature from a disordered phase to the micellar phase.

In Fig. 6 we display ε_c for different sequences as a function of the gradient strength in the copolymer. We observe that for the quenched model, the critical interaction strength (critical temperature) decreases linearly with an increase in the gradient strength of the copolymers. We note that such a trend agrees *quantitatively* with the linear dependence of the cloud point temperature as a function of the gradient strength found in the experiments of Gallow *et al.*[25,26] In the experiments, the cloud point was determined as the temperature at which the polymer solution underwent a transition from a transparent to turbid solution. Based on the similarities in the gradient strength dependence noted between our simulation results and the experiments, we conclude that the transition noted in the experiments indeed corresponds to a change from the homogeneous solution to an aggregated micellar phase.

In comparing the results for the annealed model against the quenched polymers, we observe that significantly higher critical interaction energies are required to collapse copolymers having annealed sequences. Such a result is easy to understand since the annealed model smears out the interactions between the monomers (*cf.* Fig. 2) and hence much stronger effective interactions are needed for chain collapse. This feature becomes more prominent at lower gradient strengths since, in such a limit, the identity and the interactions of the monomers becomes more uniform ($f \approx 0.5$, *cf.* Fig. 1(b)) in the annealed model and hence much higher interaction strengths are required to achieve aggregation. In contrast, the quenched model retains the specific identities and interactions of the monomers, and thus some chains possess long enough sequences of B segments to cause the collapse of the chains at much smaller interaction strengths.

What is the origin of the above-observed dependence of the critical temperature on the gradient strength? We note that the average compositions of the different copolymers considered in

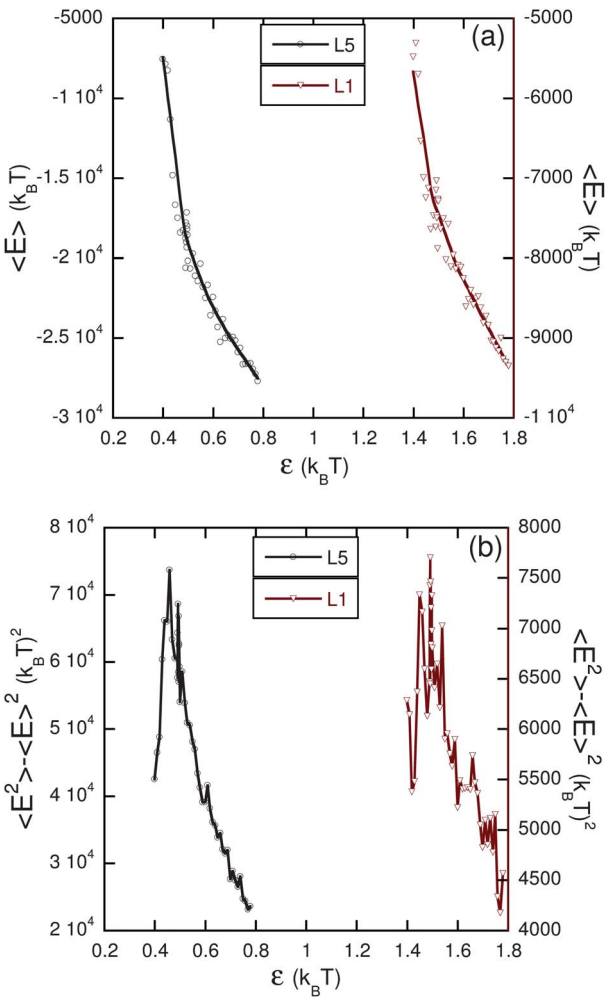

Fig. 5 Annealed model: (a) average energy and (b) average fluctuations in energy as a function of interaction parameter ε: L1 ($\Delta g = 0.2$), L5 ($\Delta g = 1.0$.) Lines are just a guide to the eye.

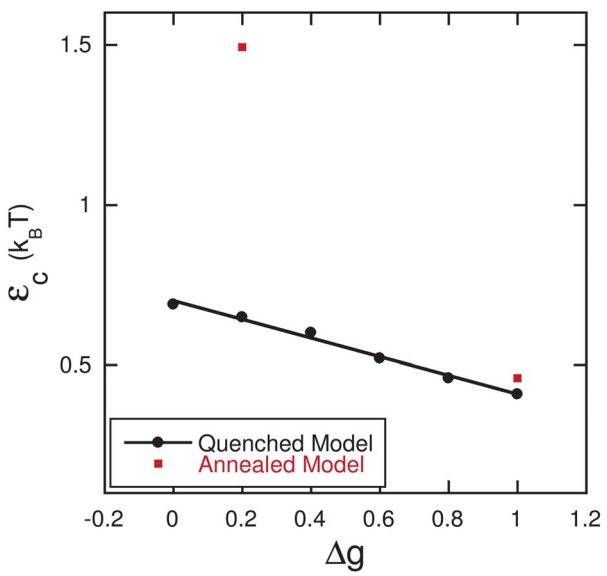

Fig. 6 Effect of gradient strength on phase transition temperature. The continuous line represents a linear fit to the data.

our study are identical and hence a mean-field (Flory–Huggins) like theory would actually predict no difference in the transition temperatures for the different systems. The latter suggests that the observed simulation results arise from correlation effects embodied in the sequences of our different gradient copolymer systems. Specifically, we hypothesize that copolymers with larger gradient strengths are more likely to possess longer sections of hydrophilic and hydrophobic groups at their ends. The presence of such longer sections of the groups would facilitate easier intermolecular aggregation of the chains and hence require only weaker interaction energies. In contrast, copolymers with weaker gradient strengths are expected to possess shorter sections of the hydrophilic and hydrophobic groups, such that aggregation would result in energetically unfavorable contacts between A and B monomers, thereby requiring stronger interaction strengths to facilitate phase separation.

In Fig. 7 and Fig. 8, we provide quantitative evidence supporting our above hypothesis. Specifically, in Fig. 7 we display the distribution of the number of blocks of continuous hydrophobic or hydrophilic monomers as a function of the gradient strength of the copolymer sequences. It can be seen that with an increase in the gradient strength, the overall distribution develops a more prominent tail towards larger blocks of continuous hydrophobic monomers. In Fig. 8 we provide a more direct measure of the block length distributions by depicting the average hydrophobic block length L_{BB} for the different polymers considered in our study. It is seen that indeed the average hydrophobic block length increases with increasing gradient strength (with the minimum occurring for $\Delta g = 0$ in the case of a purely random copolymer).

To probe whether the above trends can quantitatively explain the behavior of the critical interaction strengths observed in our simulations, we display the product of critical interaction energies and the average hydrophobic block length of such continuous hydrophobic segments in Fig. 8. It is seen that to a good degree of approximation, such a product is independent of the gradient strength, suggesting that the linear dependence of the critical interaction temperature upon the gradient strength arises purely as a consequence of the variations in the average hydrophobic block length as a function of the gradient strength.

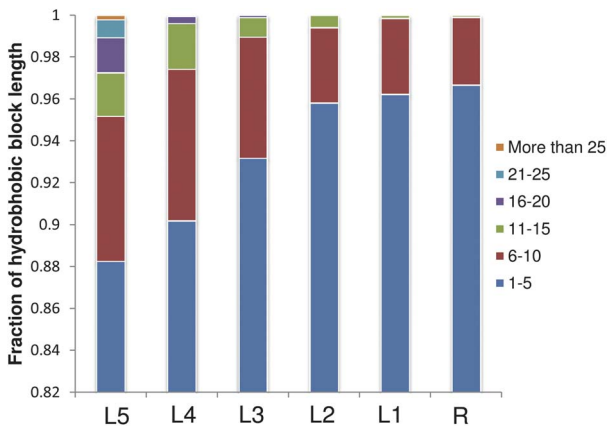

Fig. 7 Hydrophobic block length distributions for linear gradient copolymers of varying gradient strengths.

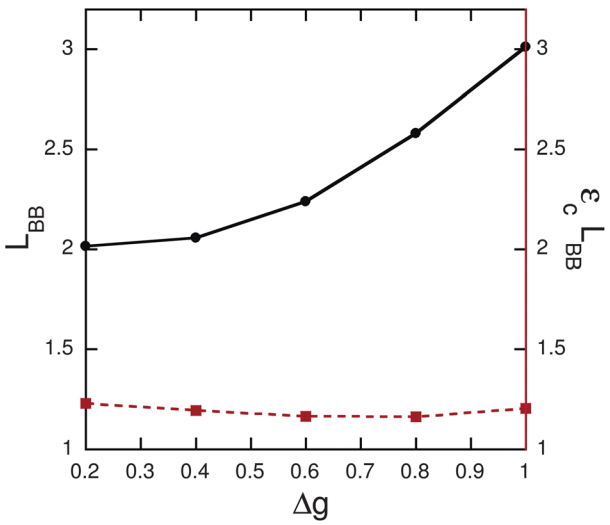

Fig. 8 Variation of average hydrophobic block length (L_{BB}) and $\varepsilon_c L_{BB}$ (dotted lines) with gradient strength for linear gradient copolymers. Lines are just a guide to the eye.

Motivated by the success of the ability of L_{BB} to quantitatively predict our simulation results for the critical interaction strengths, we probe whether similar considerations can also be used, at a quantitative level, to rationalize experimental observations. To probe this hypothesis in the context of the linear gradient copolymers studied in the experiments, we generated sequences corresponding to the experimental conditions ($f \approx 0.65$) and computed the L_{BB} corresponding to such sequences. In Fig. 9, we display a comparison of the L_{BB}^{-1} and the critical temperatures observed in the system (we assume that the cloud point temperature of the experiments T_c can be translated

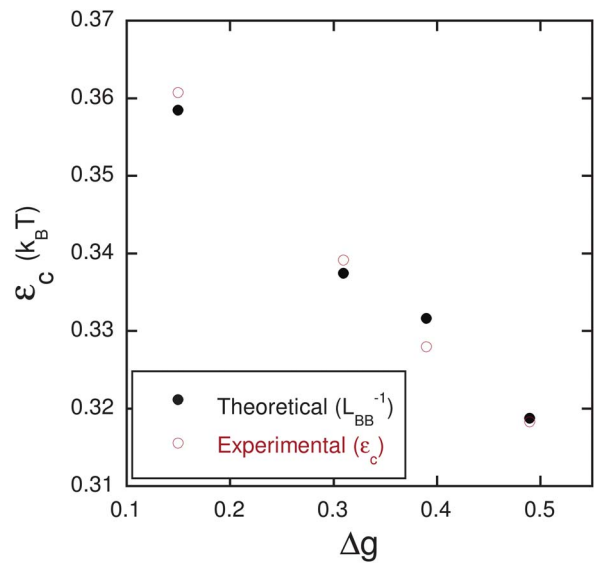

Fig. 9 Experimental and theoretical data for linear composition profile with gradient strength. Hollow points correspond to experimental data[26] normalized to fit the scale assuming $\varepsilon_c = a + bT_c$ for LCST systems. The theoretical data for ε_c correspond to inverse of average hydrophobic block length (L_{BB}).

to an interaction parameter ε_c through $\varepsilon_c = a + bT_c$, where a and b are temperature, gradient strength independent constants). In Fig. 9, it is seen that there is remarkably good agreement between T_c and the average length of the hydrophobic segments in the sequences. This quantitative agreement between the experimental work and our simulations points to the fact that L_{BB} is directly correlated with the experimentally tunable variable of gradient strength.

Experimental studies cited in the introduction have observed that a strong dependence of cloud point with gradient strength held true even for copolymers containing hyperbolic composition profiles.[26] Despite the fact that the correlation deduced in our simulations was for linear gradient copolymeric systems (and compared to the corresponding experiments above), we probe whether similar considerations ($\varepsilon \propto L_{BB}^{-1}$) hold true even when other composition profiles are considered. To achieve this, we again generated sequences corresponding to the experimental conditions of the hyperbolic gradient composition profiles and computed L_{BB} for such systems. In Fig. 10, we display a comparison of the L_{BB} and the critical temperatures observed in the system. Yet again, there is seen to be an excellent agreement between T_c and the average length of the hydrophobic segments in the sequences, suggesting that the quantity L_{BB} serves more generally as a quantitative predictor of the cloud point temperature for gradient copolymer solutions.

3.2 Intra- and intermolecular aggregation

The results presented in the preceding section provide evidence for the occurrence of a phase transition in the gradient copolymer systems. While the low temperature phase in the different copolymeric systems is well-defined as corresponding to a solution of homogeneous non-aggregated chains, the morphology of the high temperature "aggregated" systems corresponds in fact to a variety of states, ranging from a few micelles to a large network of micellar cores linked by bridges. Of interest are the questions, what is the sequence of aggregation events accompanying phase transition? Specifically, does intramolecular aggregation precede intermolecular aggregation or *vice versa*? Is there a dependence of such features on the gradient strength? For instance, in the experiments discussed in the introduction,[26] the phase transition phenomena in gradient copolymer solutions were studied by two different techniques: DLS and turbidity measurements. The former was argued to be sensitive to intrachain aggregation, whereas the latter was more sensitive to larger scale, interchain aggregation. Based on systematic differences between the aggregation temperature and the macroscopic cloud point temperature extracted from DLS and turbidity measurements, respectively, phase separation in gradient copolymer solutions was found to proceed in a two step manner wherein the intrachain aggregation occurs at a much lower temperature compared to the interchain aggregation. A specific objective of this section is to quantify the aggregation events in our simulations of gradient copolymer solutions and verify the hypothesis presented in the experimental context.

To study the above issues, we probed the temperature (interaction parameter) dependence of inter- and intramolecular BB contacts (Fig. 11) for the quenched and annealed models (not displayed). From the data in Fig. 11, it is seen that even at the lowest ε we probed, a substantial number of intrachain contacts are already present. Moreover, with an increase in ε, there is a gradual enhancement of intrachain BB contacts. In contrast, the number of interchain BB contacts is negligible at the lowest temperatures and exhibits a sharp jump at around the critical (cloud-point) temperature. Interestingly, the results for the intra- and intermolecular BB contacts for the annealed model also exhibited trends similar to that noted for the quenched model (not displayed).

The above results are qualitatively consistent with the hypothesis presented in the corresponding experiments.[26] Indeed, our results confirm that the phase transition phenomena discerned in the previous section (which we argued to correspond to the turbidity of the solution) does indeed coincide with the onset of significant interchain aggregation. However, within the limited temperature range we probed, we did not see any sharp jump in the intrachain contacts. In contrast, since the intrachain aggregation and contacts are even significant much prior to the phase transition temperature, one may conclude that the onset of intrachain aggregation occurs at a much lower ε, as was deduced through the experimental DLS measurements.

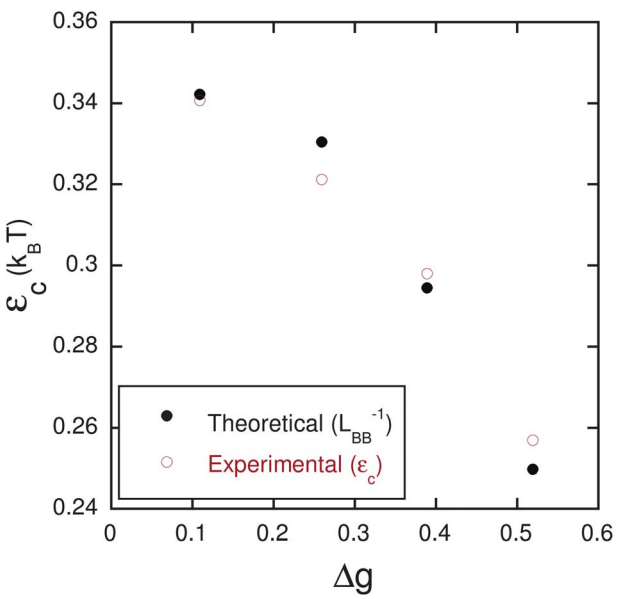

Fig. 10 Experimental and theoretical data for hyperbolic composition profile with gradient strength. Hollow points correspond to experimental data[26] normalized to fit the scale assuming $\varepsilon_c = a + bT_c$ for LCST systems. The theoretical data for ε_c correspond to inverse of average hydrophobic block length (L_{BB}).

3.3 Interaggregate bridges

The preceding two sections provided evidence for the influence of the gradient strength upon the phase transition temperature and the nature of the accompanying transition. In this final section, we discuss the influence of the gradient strength on the nature of the aggregates and the larger lengthscale structures formed subsequent to the phase separation. The results presented in this section are motivated by the results of experimental transmittance studies which revealed a larger breadth of transition (*i.e.* temperature interval over which the copolymer solution

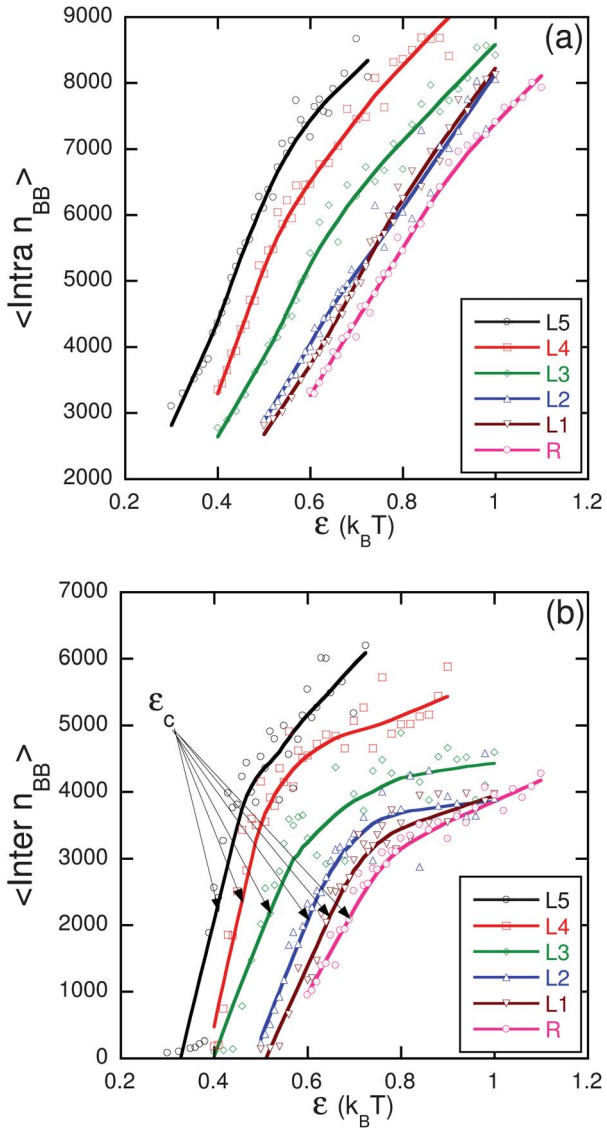

Fig. 11 Average number of BB contacts for quenched model: (a) Intramolecular (b) Intermolecular as a function of interaction parameter ε: R ($\Delta g = 0$), L1 ($\Delta g = 0.2$), L2 ($\Delta g = 0.4$), L3 ($\Delta g = 0.6$), L4 ($\Delta g = 0.8$), L5 ($\Delta g = 1.0$). Lines are just a guide to the eye.

changes from transparent to turbid[25]) for higher gradient strength copolymers. We hypothesize that such results arise from the fact that lower gradient strength copolymers possess shorter sequences of hydrophobic (B) groups (*cf.* Fig. 8), and also are more likely to possess B groups towards the middle and A-rich regions of the chains. As a consequence, we propose that the lower (higher) gradient strength copolymers tend to form smaller (larger) sized aggregates, but with substantially more (less) intermicellar connections (bridges). Since the formation of bridges corresponds to the growth of larger length scale structures, we associate the breadth of the transition noted in the transmittance experiments to the number of bridges as a function of temperature and gradient strengths. To corroborate these hypotheses, in this section we present results which characterize the micellar aggregates through two measures: (i) their aggregation numbers (*i.e.* number of monomers in the micellar core); and (ii) the bridging number, which quantifies the number of chains forming bridges between micelles relative to the total number of chains. A chain is identified as forming a bridge if its hydrophobic monomers belong to at least two different micelle cores.

In Fig. 12(a), we display the results for aggregation number of the micelles as a function of the gradient strength in the copolymers. Consistent with the hypothesis presented above, we indeed observe that the aggregation numbers decrease with decreasing gradient strengths. To compare these results with the behavior of annealed model copolymer sequences, we also display the aggregation numbers for L1 and L5 using the annealed model in Fig. 12(b). In contrast to the trends noted for the quenched

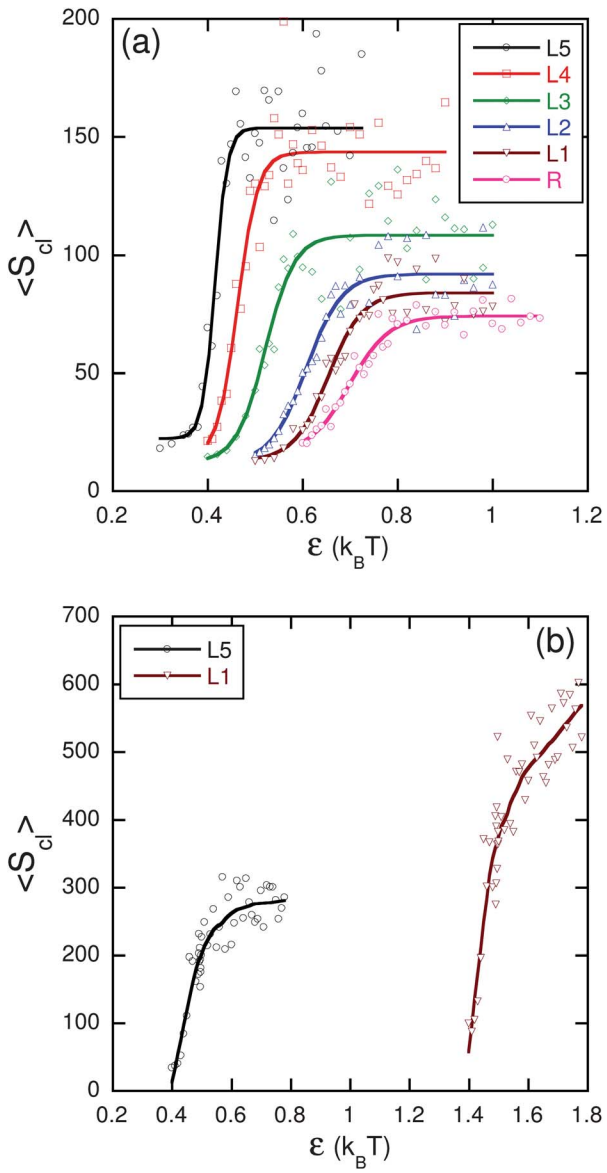

Fig. 12 (a) Change in average size of micelle core with interaction parameter ε: R ($\Delta g = 0$), L1 ($\Delta g = 0.2$), L2 ($\Delta g = 0.4$), L3 ($\Delta g = 0.6$), L4 ($\Delta g = 0.8$), L5 ($\Delta g = 1.0$). (b) Size of cluster for annealed model as a function of interaction parameter ε: L1 ($\Delta g = 0.2$), L5 ($\Delta g = 1.0$). Lines are just a guide to the eye.

model, the aggregation numbers are found to increase with decreasing gradient strength in the annealed model. These results are easy to understand in the context that the annealed model becomes akin to a homopolymer solution (in a poor solvent) in the limit of weak gradient strengths of the copolymer. Hence, at interaction strengths greater than the critical value, the system undergoes macroscopic phase separation characterized by the formation of a large aggregates which represent intermediates in the path towards a completely segregated system.

In Fig. 13, we display the bridging numbers in the micelles as a function of the gradient strength of the copolymers. In accord with our hypothesis above, it can be seen that both the number of chains forming bridges, as well as the sharpness of the temperature dependence of the number of bridges, correlates inversely with the gradient strength of the copolymer solutions sequences. This result is physically intuitive since the weakest gradient copolymers are more likely to possess smaller blocks of hydrophobic monomers which are distributed over the entire backbone (*cf.* Fig. 8). Such blocks are more likely to become involved in independent aggregation events with other chains and result in the formation of bridges among neighboring chains. Indeed, the stronger gradient copolymers resemble diblock copolymers due to their blocky ends, and hence the number of chains forming bridges are substantially lowered in such systems.

4 Conclusion

By using MC simulations and a parallel tempering algorithm, we have studied the phase behavior of amphiphilic linear gradient copolymers for both quenched and annealed models of sequences. Under poor solvent conditions, the copolymer chains collapse to form micelle-like structures. With the quenched model, we found a linear trend for transition temperature with gradient strength which agrees with the results reported by Gallow *et al.*[25] We argued that such trends arise from the average length of the hydrophobic segments L_{BB} in the gradient copolymer sequences. After validating this hypothesis against our simulation results for linear gradient copolymers, we demonstrated that L_{BB} provides a quantitative means to predict the cloud point temperatures of gradient copolymer solutions even for other composition profiles.

As a second aspect of this work, we probed the statistics of the aggregates formed during the phase separation process and confirmed the two-step sequence of aggregation hypothesized in experiments. Specifically, interchain interactions were found to undergo a sudden jump around the critical (cloud point) temperature, whereas the onset of intrachain aggregation occurred at much lower interaction strengths, consistent with the observation of a unimer-to-aggregate transition *via* DLS at temperatures below the macroscopic cloud points. A strong dependence of the resulting micellar properties upon the gradient strength of copolymers was also observed.

In this work, we also contrasted our results for the quenched model of gradient copolymer against that of the annealed model. In the latter situation, due to smearing of interactions, the copolymer collapse occurred at a significantly higher interaction strength as compared to quenched model. While the annealed model exhibited a similar sequence of aggregation events as the quenched model, much of the behaviors upon varying the gradient strengths either disappeared or contrasted with the quenched model due to the lack of sequence correlations in the annealed model.

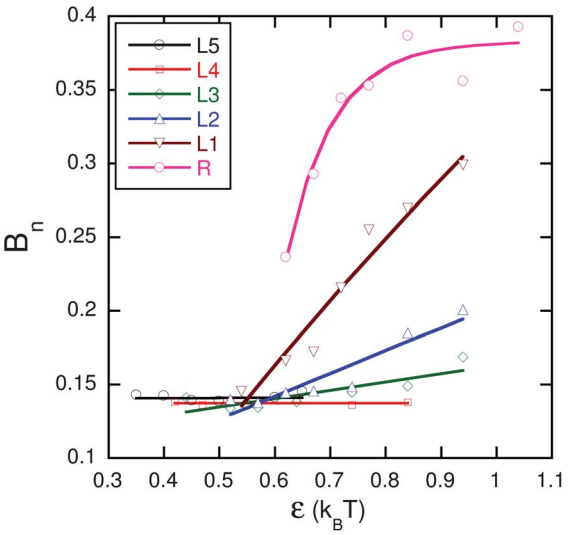

Fig. 13 The variation in bridge number, B_n with gradient strength, Δg. Lines are just a guide to the eye.

Acknowledgements

This work was supported by the National Science Foundation (1005739), the National Science Foundation's Partnerships for International Research and Education (NSF-PIRE 0730243), a grant from the Robert A. Welch Foundation (Grant F1599) and the US Army Research Office under grant W911NF-10-10346. The authors acknowledge the Texas Advanced Computing Center (TACC) at The University of Texas at Austin for providing computing resources that have contributed to the research results reported within this paper.

References

1 F. S. Bates and G. H. Fredrickson, *Annu. Rev. Phys. Chem.*, 1990, **41**, 525–557.
2 M. T. Krejchi, E. D. T. Atkins, A. J. Waddon, M. J. Fournier, T. L. Mason and D. A. Tirrell, *Science*, 1994, **265**, 1427–1432.
3 S. J. M. Yu, V. P. Conticello, G. H. Zhang, C. Kayser, M. J. Fournier, T. L. Mason and D. A. Tirrell, *Nature*, 1997, **389**, 167–170.
4 M. J. Fasolka and A. M. Mayes, *Annu. Rev. Mater. Res.*, 2001, **31**, 323–355.
5 C. J. Hawker, A. W. Bosman and E. Harth, *Chem. Rev.*, 2001, **101**, 3661–3688.
6 S. Aoshima, S. Sugihara, M. Shibayama and S. Kanaoka, *Macromol. Symp.*, 2004, **215**, 151–163.
7 G. Moad, E. Rizzardo and S. H. Thang, *Polymer*, 2008, **49**, 1079–1131.
8 K. Matyjaszewski and N. V. Tsarevsky, *Nat. Chem.*, 2009, **1**, 276–288.
9 M. Dadmun, *Macromolecules*, 1996, **29**, 3868–3874.
10 T. E. Patten and K. Matyjaszewski, *Adv. Mater.*, 1998, **10**, 901–915.
11 J. Kim, M. K. Gray, H. Y. Zhou, S. T. Nguyen and J. M. Torkelson, *Macromolecules*, 2005, **38**, 1037–1040.
12 C. L. H. Wong, J. Kim, C. B. Roth and J. M. Torkelson, *Macromolecules*, 2007, **40**, 5631–5633.
13 J. Kim, R. W. Sandoval, C. M. Dettmer, S. T. Nguyen and J. M. Torkelson, *Polymer*, 2008, **49**, 2686–2697.

14 R. Malik, C. K. Hall and J. Genzer, *Soft Matter*, 2011, **7**, 10620–10630.
15 M. Kryszewski, *Polym. Adv. Technol.*, 1998, **9**, 244–259.
16 U. Beginn, *Colloid Polym. Sci.*, 2008, **286**, 1465–1474.
17 Y. Sha, C. Y. Hui, E. J. Kramer, S. F. Hahn and C. A. Berglund, *Macromolecules*, 1996, **29**, 4728–4736.
18 J. Kim, M. M. Mok, R. W. Sandoval, D. J. Woo and J. M. Torkelson, *Macromolecules*, 2006, **39**, 6152–6160.
19 S. Jouenne, J. A. Gonzalez-Leon, A. V. Ruzette, P. Lodefier, S. Tence-Girault and L. Leibler, *Macromolecules*, 2007, **40**, 2432–2442.
20 P. Hodrokoukes, G. Floudas, S. Pispas and N. Hadjichristidis, *Macromolecules*, 2001, **34**, 650–657.
21 S. Okabe, K. Seno, S. Kanaoka, S. Aoshima and M. Shibayama, *Polymer*, 2006, **47**, 7572–7579.
22 S. Okabe, K. Seno, S. Kanaoka, S. Aoshima and M. Shibayama, *Macromolecules*, 2006, **39**, 1592–1597.
23 R. Hoogenboom, H. M. L. Lambermont-Thijs, M. J. H. C. Jochems, S. Hoeppener, C. Guerlain, C. A. Fustin, J. F. Gohy and U. S. Schubert, *Soft Matter*, 2009, **5**, 3590–3592.
24 N. Merlet-Lacroix, E. Di Cola and M. Cloitre, *Soft Matter*, 2010, **6**, 984–993.
25 K. C. Gallow, Y. K. Jhon, W. Tang, J. Genzer and Y.-L. Loo, *Journal Of Polymer Science Part B-Polymer Physics*, 2011, **49**, 629–637.
26 K. C. Gallow, Y. K. Jhon, J. Genzer and Y.-L. Loo, *Polymer*, 2012, **53**, 1131–1137.
27 A. Aksimentiev and R. Holyst, *Progress In Polymer Science*, 1999, **24**, 1045–1093.
28 M. D. Lefebvre, M. O. de la Cruz and K. R. Shull, *Macromolecules*, 2004, **37**, 1118–1123.
29 R. Jiang, Q. H. Jin, B. H. Li, D. T. Ding, R. A. Wickham and A. C. Shi, *Macromolecules*, 2008, **41**, 5457–5465.
30 R. Wang, W. H. Li, Y. W. Luo, B. G. Li, A. C. Shi and S. P. Zhu, *Macromolecules*, 2009, **42**, 2275–2285.
31 N. B. Tito, S. T. Milner and J. E. G. Lipson, *Macromolecules*, 2010, **43**, 10612–10620.
32 T. Pakula and K. Matyjaszewski, *Macromolecular Theory And Simulations*, 1996, **5**, 987–1006.
33 K. R. Shull, *Macromolecules*, 2002, **35**, 8631–8639.
34 G. T. Pickett, *Journal Of Chemical Physics*, 2003, **118**, 3898–3903.
35 D. M. Trombly and V. Ganesan, *Journal of Chemical Physics*, 2010, **133**, 154904–1.
36 D. M. Trombly, V. Pryamitsyn and V. Ganesan, *Macromolecules*, 2011, **44**, 9867–9881.
37 D. M. Trombly, V. Pryamitsyn and V. Ganesan, *Physical Review Letters*, 2011, **107**, 148304–1.
38 D. M. Trombly, V. Pryamitsyn and V. Ganesan, *Journal of Chemical Physics*, 2011, **134**, 154903–1.
39 Y. A. Kuznetsov, E. G. Timoshenko and K. A. Dawson, *Journal Of Chemical Physics*, 1995, **103**, 4807–4818.
40 J. M. P. van den Oever, F. A. M. Leermakers, G. J. Fleer, V. A. Ivanov, N. P. Shusharina, A. R. Khokhlov and P. G. Khalatur, *Physical Review E*, 2002, **65**, 041708–1.
41 A. R. Khokhlov and P. G. Khalatur, *Physica A*, 1998, **249**, 253–261.
42 A. R. Khokhlov and P. G. Khalatur, *Physical Review Letters*, 1999, **82**, 3456–3459.
43 T. M. Beardsley and M. W. Matsen, *European Physical Journal E*, 2010, **32**, 255–264.
44 K. Lewandowski and M. Banaszak, *Physical Review E*, 2011, **84**, 011806–1.
45 J. Houdayer and M. Muller, *Macromolecules*, 2004, **37**, 4283–4295.
46 A. Cavallo, M. Muller and K. Binder, *Macromolecules*, 2006, **39**, 9539–9550.
47 K. Binder and W. Paul, *Macromolecules*, 2008, **41**, 4537–4550.
48 B. M. Baysal and F. E. Karasz, *Macromolecular Theory And Simulations*, 2003, **12**, 627–646.
49 O. N. Vassiliev and M. W. Matsen, *Journal Of Chemical Physics*, 2003, **118**, 7700–7713.
50 T. Pakula, K. Karatasos, S. H. Anastasiadis and G. Fytas, *Macromolecules*, 1997, **30**, 8463–8472.
51 H. P. Deutsch and K. Binder, *Journal Of Chemical Physics*, 1991, **94**, 2294–2304.
52 W. Jilge, C. I, K. Kremer and K. Binder, *Macromolecules*, 1990, **23**, 5001–5013.
53 M. Muller, K. Binder and W. Oed, *Journal Of The Chemical Society-Faraday Transactions*, 1995, **91**, 2369–2379.
54 A. Hoffmann, J. U. Sommer and A. Blumen, *Journal Of Chemical Physics*, 1997, **106**, 6709–6721.
55 H. Weber and W. Paul, *Physical Review E*, 1996, **54**, 3999–4007.
56 V. Pryamitsyn, B. Hanson and V. Ganesan, *Macromolecules*, 2011, **44**, 9839–9851.
57 N. Metropolis, A. Rosenbluth, M. Rosenbluth, A. Teller and E. Teller, *Journal of Chemical Physics*, 1953, **21**, 1087–1092.
58 J. P. Wittmer, A. Cavallo, T. Kreer, J. Baschnagel and A. Johner, *Journal of Chemical Physics*, 2009, **131**, 064901.
59 K. Hukushima and K. Nemoto, *Journal Of The Physical Society Of Japan*, 1996, **65**, 1604–1608.
60 D. Frenkel and B. Smit, *Understanding Molecular Simulation, Second Edition: From Algorithms to Applications (Computational Science)*, Academic Press, 2nd edn, 2001.
61 Y. H. Li, M. Mascagni and A. Gorin, *Parallel Computing*, 2009, **35**, 269–283.
62 M. Mascagni and A. Srinivasan, *Acm Transactions On Mathematical Software*, 2000, **26**, 618–619.
63 M. Surve, V. Pryamitsyn and V. Ganesan, *Physical Review Letters*, 2006, **96**, 177805–1.
64 M. Surve, V. Pryamitsyn and V. Ganesan, *Langmuir*, 2006, **22**, 969–981.
65 C. V. Mahajan and V. Ganesan, *Journal of Physical Chemistry B*, 2010, **114**, 8357–8366.
66 E. M. Sevick, P. A. Monson and J. M. Ottino, *Journal Of Chemical Physics*, 1988, **88**, 1198–1206.

Addition and correction

Note from RSC Publishing

This article was originally published with incorrect page numbers. This is the corrected, final version.

The Royal Society of Chemistry apologises for these errors and any consequent inconvenience to authors and readers.